

The Devil is in the Spurious Correlation: Boosting Moment Retrieval via Temporal Dynamic Learning

Xinyang Zhou^{1*} Fanyue Wei^{1,2*} Lixin Duan¹ Wen Li¹

¹University of Electronic Science and Technology of China ²National University of Singapore

{x.y.zhou2020, wfanyue, liwenbnu, lxduan}@gmail.com

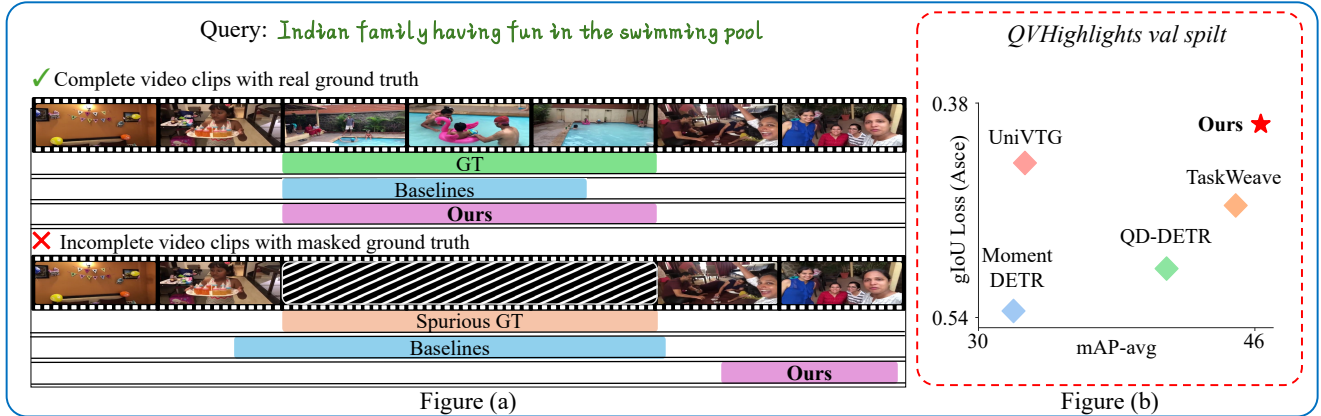


Figure 1. (a) Comparison of moment retrieval models under normal and spurious correlation videos by masking the content of target clips of video. We found the existing work suffering from a crucial reason stems from the spurious correlation between the text queries and the moment context. Baselines predict the Spurious GT even if the target moments are masked. In contrast, *TD-DETR* predicts the second-best moments with lower confidence. (b) Our model achieves the best ratio of mAP to gIoU loss.

Abstract

Given a textual query along with a corresponding video, the objective of moment retrieval aims to localize the moments relevant to the query within the video. While commendable results have been demonstrated by existing transformer-based approaches, predicting the accurate temporal span of the target moment is currently still a major challenge. In this paper, we reveal that a crucial reason stems from the spurious correlation between the text queries and the moment context. Namely, the model may associate the textual query with the background frames rather than the target moment. To address this issue, we propose a temporal dynamic learning approach for moment retrieval, where two strategies are designed to mitigate the spurious correlation. First, we introduce a novel video synthesis approach to construct a dynamic context for the relevant moment. With separate yet similar videos mixed up, the synthesis approach empowers our model to attend to the target moment of the corresponding query under various dynamic

contexts. Second, we enhance the representation by learning temporal dynamics. Besides the visual representation, text queries are aligned with temporal dynamic representations, which enables our model to establish a non-spurious correlation between the query-related moment and context. With the aforementioned proposed method, the spurious correlation issue in moment retrieval can be largely alleviated. Our method establishes a new state-of-the-art performance on two popular benchmarks of moment retrieval, i.e., *QVHighlights* and *Charades-STA*. In addition, the detailed ablation analyses demonstrate the effectiveness of the proposed strategies. Our code will be publicly available.

1. Introduction

As digital platforms become increasingly integrated into people’s lives, videos have emerged as one of the most sought-after media formats for users [9, 35, 48]. However, browsing through entire videos is time-consuming, making it cumbersome to localize moments relevant to a natural language sentence description [1, 59].

*Equal contribution.

Using a textual description to retrieve corresponding moments within a given lengthy video plays an important role in various aspects such as entertainment, information search and *etc.*, which attracts increasing interest from the research community. Existing approaches [17, 18, 20, 33, 53] leverage detection transformer (DETR) [3] framework to model the relationship of text and vision tokens for moment retrieval. Moment-DETR [20] employs a DETR-manner to model the relationship of video segments, while UMT [30] integrates the text queries in the transformer decoder and QD-DETR [33] focused on the video-text interaction and highlight detection. Besides, BM-DETR [17] adopts a contrastive approach by the negative queries alignment with other moments in the video. Recently, TaskWeave [53] investigated the interplay between moment retrieval and highlight detection.

Although existing transformer-based approaches have shown remarkable results, accurately predicting the temporal span of the target moment remains a significant challenge. We identify that a crucial reason stems from the *spurious correlation* between the text queries and the moment context. *i.e.*, the moment retrievers tend to associate the textual query with the background frames rather than the target moment. As illustrated in Figure 1, to localize the “Indian family having fun in the swimming pool” within the given video, even when the target moment is masked, the existing method still predicts a similar span, whereas it ought to output an alternative reasonable span relevant to text queries. Such issues lead to a sub-optimal performance for moment retrieval, as illustrated by sub-figure (b) in Figure 1.

In addition, the visual representation is aligned with the semantics of the text in the cross-attention module, thus generally containing appearance or spatial information. Consequently, the semantic elements in background frames are overly associated with textual queries, which can amplify the spurious correlation.

To address the aforementioned issues, we propose a temporal dynamic learning approach for moment retrieval, where two strategies are designed to mitigate the spurious correlation. First, we introduce a novel video synthesizer to dynamically contextualize target moments for retrieval. By selecting spurious similar video pairs to synthesize a new video with dynamic context for the target moment, the synthesis approach enables our framework to attend to the target moment of the corresponding query under various dynamic contexts. Second, we also propose to enhance representations with temporal dynamics by aligning the text queries with temporal dynamic representations. We design a simple yet efficient tokenizer to derive the temporal dynamic representation. Followed by a text-dynamic interactor to leverage the dynamic representation with text queries, which enables our model to establish a non-spurious correlation with complementary representations.

With the proposed strategies, the *spurious correlation* in moment retrieval can be largely alleviated. Experiments on two challenging benchmarks, *i.e.*, QVHighlights and Charades-STA, show that our method outperforms existing methods by clear margins. Moreover, the detailed ablation analyses demonstrate the effectiveness of the proposed strategies.

In conclusion, our contributions to this work are summarized as follows:

- To the best of our knowledge, we are the first to investigate the spurious correlation in moment retrieval.
- We propose a temporal dynamic learning approach for moment retrieval that mitigates spurious correlations by dynamically contextualizing target moments through novel video synthesis and enhancing representations with aligned temporal dynamics.
- The proposed method achieves state-of-the-art performance across all benchmarks. Furthermore, our model also provides a strong interpretation of *spurious* correlations.

2. Related Work

2.1. Moment Retrieval

Moment Retrieval aims to predict a temporal span within a video based on a given natural language query [59]. This area has been extensively studied in recent years. Early methods primarily employed an inefficient two-stage approach, which involved sampling candidate moments as proposals and subsequently scoring them to obtain the final predictions [1, 10, 11, 26, 27]. However, more recent research has shifted towards more effective and end-to-end approaches [5, 6, 22, 25, 32, 40, 43, 49–51, 54, 55, 57, 61, 62, 65, 66]. TGN [5] utilized Recurrent Neural Networks (RNNs) to generate a set of proposals with varying lengths. SCDM [54] and MAN [57] employed convolution to expand the receptive field while Feature Pyramid Networks (FPN) [24] were used to generate multi-scale proposals. 2D-TAN [62] instead enumerated all possible spans using a sparse sampling strategy. In contrast, proposal-free methods directly predict the start and end points, or their associated probabilities, eliminating the need for pre-designed proposals and thereby reducing computational costs. DRN [56] utilized three convolutional modules to predict video-text matching scores, Intersection over Union (IoU), and spans. XML [19] first computes the text-video similarity and then predicts scores of clips using convolutional layers followed by softmax. Although many methods in moment retrieval have achieved remarkable performance, most of them overlook the issue of spurious correlations, which is addressed in the following subsection (2.3). In contrast, our work proposes a novel temporal dynamic learning to tackle this problem.

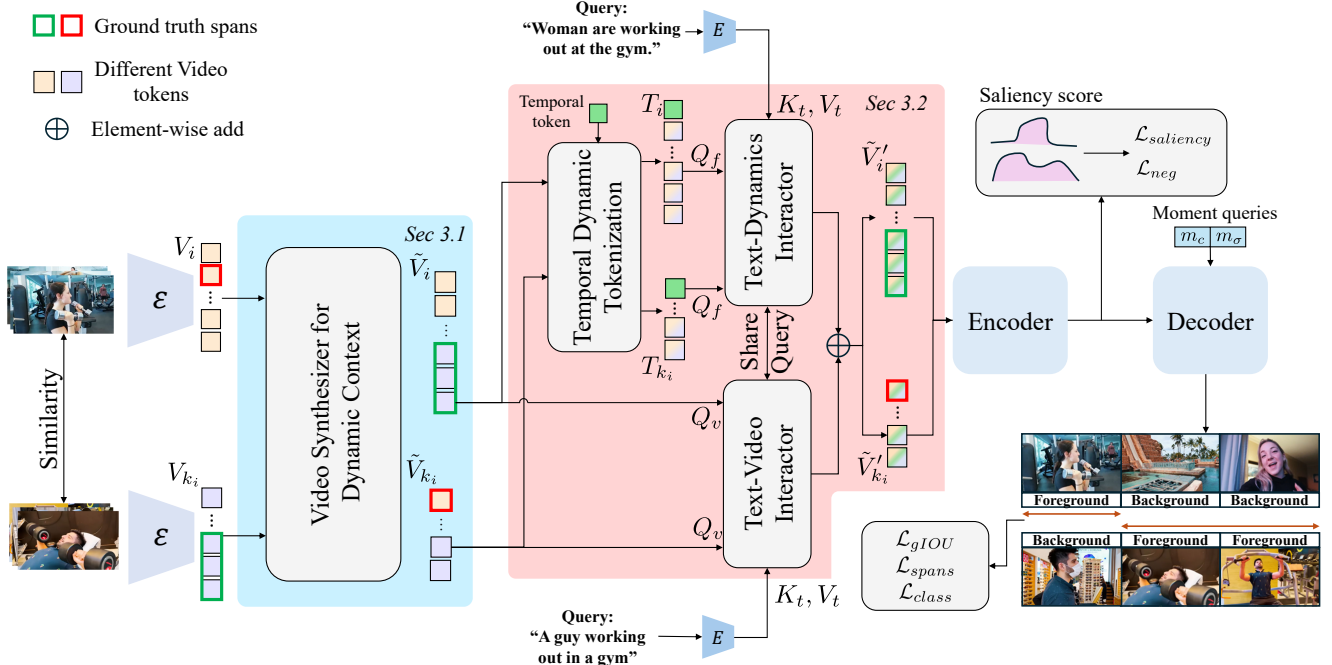


Figure 2. Overview of the proposed *TD-DETR*. Video pairs are sampled by their similarity and then forwarded into the Video Synthesizer to generate Dynamic Context (Section 3.1), Then, the Dynamic Context, *i.e.*, synthesized pairs, are enhanced by Temporal Dynamic Tokenization and interact with textual information (Section 3.2). Finally, the enhanced video tokens are sent to the transformer encoder-decoder with prediction heads to predict moments (Section 3.3).

2.2. Detection Transformers

In the past several years, the wide adoption of detection transformers (DETR) [3] in video moment retrieval has gained remarkable performance [16, 18, 20, 28–30, 33, 52, 53, 67]. While introducing the DETR framework to the task of moment retrieval, it demonstrated the effectiveness on QVHighlights.dataset [20]. Subsequently, UMT [30] emphasized the importance of multimodal feature fusion, while QD-DETR [33] highlighted the crucial role of natural language queries in improving result prediction. BAM-DETR [18] addressed the issue of center misalignment, and TaskWeave [53] explored the relationship between moment retrieval and highlight detection. Our work is closely related to DETR-based approaches. Notably, our architecture is compatible with any moment retrieval network and can be enhanced with temporal dynamic learning to improve model robustness and mitigate the impact of spurious correlations.

2.3. Spurious Correlation

In recent years, researchers have increasingly recognized that vision algorithms often suffer from poor generalization, relying on memorized patterns or contextual cues that lead to low accuracy on rare or atypical test samples [2, 12, 13, 15, 42, 45]. Thus, *Spurious Correla-*

tions was introduced to the vision area: misleading heuristics imbibed within the training dataset that is correlated with the majority of examples but does not hold in general [13]. Numerous approaches have been proposed to address this challenge, aiming to improve performance and robustness across various domains, including computer vision, natural language processing, action detection, and more [36, 46, 47, 59, 60, 63, 64]. In Moment Retrieval, [36] investigates the biases introduced by text queries and the neglect of semantic information, while [59] explores the distribution of start and end moments. Despite the previous works [18, 36, 59] in Moment Retrieval discussed the inherent bias in the dataset, they ignore the problem of spurious correlation in context and semantic alignment between videos and text queries, which is a key challenge of moment retrieval. We focus on these parts and develop a new method to alleviate this problem.

3. Methodology

The objective of moment retrieval is to localize a temporal span that semantically corresponds to a given text query. We denote the video with L vision tokens as $V = \{v_1, v_2, \dots, v_L\}$ along with a natural language description, containing M words, as $\{q_1, q_2, \dots, q_M\}$.

The retrieval model aims to predict a temporal span m

with centre m_c and duration m_σ which is relevant to the textual query, and clip-wise saliency scores $\{s_1, s_2, \dots, s_L\}$ of the text.

Existing approaches [20, 33] adopt a DETR-like framework to localize the moment span. Despite promising advances achieved by modelling the correlation between text queries and video clips with cross-attention, existing methods still grapple with issues of *spuriousness*, leading to inaccurate temporal span prediction. To address the spurious correlation, we propose a novel framework to learn *Temporal Dynamics* utilizing *DE*tectio*TR*ansformer (**TD-DETR**) in this work.

The overview of the proposed framework is illustrated in Figure 2. To correlate the spuriousness, we introduce a novel video synthesis strategy to construct dynamic context with specific moments. Besides, we also enhance the representation with dynamics.

To distinguish the text query in moment retrieval and the query in attention mechanism, we use italic letters to represent *query*, *key*, and *value* of attention layers.

3.1. Video Synthesizer for Dynamic Context

We introduce a novel video synthesizer to infuse the target moments with dynamic context for moment retrieval. Since spurious correlations stem from the overlook of the moment’s context rather than text query, we propose to address the issue by synthesizing a new sample regarding the target moment with a more dynamic context, where the context aligns with the target moment both temporally and semantically. Thus, the model has the capability to effectively attend to the target moment corresponding to the text query, even within a dynamic context.

Spurious Pair Selection. In order to synthesize a dynamic context aligned with the target moment, we construct a spurious pair of the target moment in a given video V . To ensure the challenge and rationality of the synthesized video, we select a video which is similar to V contextually

In a training batch of N video samples, we sample a most similar video $\{V_{k_i}\}$ for every $\{V_i\}$ where $k_i \in [1, N]$, for each $i \in [1, N]$ to construct a spurious video pair p_i .

We employ cosine similarity matrix $S \in \mathbb{R}^{N \times N}$ to model the similarity relationship between videos as follows:

$$\begin{cases} a_{k,l} = \frac{1}{L_k \cdot L_l} \sum_{i=0}^{L_k} \sum_{j=0, i \neq j}^{L_l} \frac{v_i^k \cdot v_j^l}{\|v_i^k\| \cdot \|v_j^l\|}, & k, l \in [1, N]. \\ S = \{a_{k,l}\}_{1 \leq k \leq N, 1 \leq l \leq N} \end{cases} \quad (1)$$

We denote v_i^k and v_j^l i -th clip of V_k and j -th clip of V_l , L_k and L_l for the length of V_k and V_l , $a_{k,l}$ for the average similarity between V_k and V_l and S for the batch similarity matrix. We select the most similar video V_{k_i} for every video V_i by $k_i = \arg \max_{k_i \in [0, N]} S_{[i, \setminus \{i\}]}$ in the batch.

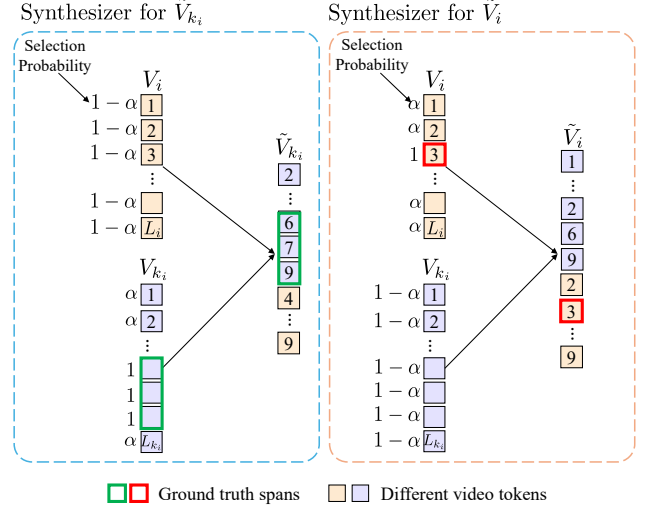


Figure 3. Illustration of Video Synthesis with Dynamic Context. The number in the boxes is the ID of the tokens and indicates the order of tokens. We sampled tokens via their selection probabilities and concatenated them.

For i -th pair, we denote the sampled subset using $p_i = \{V_i, V_{k_i}\}$

Video Synthesis with Dynamic Context. After obtaining the spurious pairs, a new video \tilde{V}_i can be synthesized with the target moment m and the spurious pair p_i (where $p_i = \{V_i, V_{k_i}\}$), we composite $\{V_i, V_{k_i}\}$ and refine ground truths of the target moment m_i dynamically. Illustrated by Figure 3, given video V_i with L_i tokens and V_{k_i} with L_{k_i} tokens, on the one hand, we expect the sample from V_i and V_{k_i} with the completeness of target moment m_i of V_i . We first sample from V_i without ground truth tokens $NG \in [0, L_i] \setminus m_i$ with sampling ratio α , *i.e.*, every token in NG has the same ratio α to be selected. We sample from the paired V_{k_i} with sampling ratio $1 - \alpha$, since V_{k_i} is irrelevant to ground truth m_i .

Finally, we concatenate the two sets of sampled video tokens into \tilde{V}_i . On the other hand, we have the same process, except now we focus on V_{k_i} and GT_{k_i} with sampling ratio α and ratio $1 - \alpha$ to sample from the whole V_i and concatenate sampled tokens into \tilde{V}_{k_i} .

3.2. Temporal Dynamics Enhancement

The attention of DETR-like architecture associates text queries with vision representation, which often emphasizes background frames, thereby exacerbating the *spurious correlation*. To this end, besides the dynamic context synthesis, we introduce a temporal dynamics enhancement module to encourage our model to align text queries with temporal dynamics representations.

Thus, the model considers not only the association of background frames but also background-independent dy-

namics. This alignment enables our model to establish a stand-up correlation between the query-related moment and its context.

Temporal Dynamic Tokenizer. To model the dynamic temporality, we introduce a simple yet effective strategy to tokenize the temporal dynamics, which is nearly cost-free to obtain temporal dynamic representations.

Given spurious pair $p_i = \{\tilde{V}_i, \tilde{V}_{k_i}\}$, the temporal dynamic tokenizer processes all video pairs in the same manner. Then, we use \tilde{V}_i to explain the processing steps without loss of generality.

First, we concatenate a learnable token to the start of the video as follows:

$$\tilde{V}_i = \{st, \tilde{v}_1, \tilde{v}_2, \dots, \tilde{v}_L\}, \quad (2)$$

where st is a learnable token that captures the start signal of the video, preventing the loss of information from the first clip in the video representations. We then employ an element-wise difference to model the temporal dynamics.

$$T = \{\tilde{v}_1 - st, \tilde{v}_2 - \tilde{v}_1, \tilde{v}_3 - \tilde{v}_2, \dots, \tilde{v}_{L_i} - \tilde{v}_{L_i-1}\}, \quad (3)$$

where T is a learnable temporal representation, it learns and focuses on the dynamic information in nearby video clips.

Text-Dynamics Interactor. The vision representation generally contains appearance or spatial information, which is necessarily aligned with the semantics of texts in cross attention module. Therefore, the semantic elements in background frames are over-associated with textual queries, the spurious correlation may be exaggerated.

To tackle such issues, we employ cross-attention layers for both text-vision representations and text-dynamics representations to enhance the representation with dynamics to mitigate the overemphasis on video context. In detail, we deploy two cross-attention layers for video-text and temporal-text modalities respectively, which means the Text-Video and Text-Dynamics Interactor share the same query *i.e.*, text. The dynamic representations can be obtained by Eq. 3 from the temporal dynamic tokenizer.

In detail, the *query* for each cross-attention layer is prepared by linear projection of the video and temporal clips as follows:

$$Q_\delta = [p_\delta(\delta), \dots, p_\delta(\delta_{L_i})], \delta \in \{\tilde{V}_i, T\}. \quad (4)$$

The *key* and *value* are computed with the query text representation as $K_t = [p_k(q_1), \dots, p_k(q_L)]$ and $V_t = [p_v(q_1), \dots, p_v(q_L)]$, p_d, p_t, p_k, p_v are linear projection layers for dynamic-enhanced *query*, temporal *query*, *key* and *value*. Then the cross-attention layer operates as follows:

$$\text{Attention}(Q_\delta, K_t, V_t) = \text{softmax}\left(\frac{Q_\delta K_t^T}{\sqrt{d}}\right)V_t, \delta \in \{\tilde{V}_i, T\}, \quad (5)$$

where d is the dimension of the projected *key*, *value* and *query*. To emphasize the learned temporal information, we utilize the weighted element-wise addition to inject text-guided temporal representation into text-guided dynamic-enhanced representation as follows:

$$\tilde{V}'_i = \beta \cdot \tilde{V}_i + (1 - \beta) \cdot T', \quad (6)$$

where β is a hyper-parameter to adapt the addition ratio between \tilde{V}_i and T' . Hence, from the spurious pair $p_i = \{\tilde{V}_i, \tilde{V}_{k_i}\}$, we obtain a new spurious pair $p'_i = \{\tilde{V}'_i, \tilde{V}'_{k_i}\}$.

3.3. Network and Objectives

As shown in Figure 2, we elucidate the network structure following the previous work [20, 33]. Due to space limitations, we recommend that readers refer to Section 6 in the supplementary materials for formulas and further details.

Transformer encoder-decoder with prediction heads. Given spurious pair $p'_i = \{\tilde{V}'_i, \tilde{V}'_{k_i}\}$, this module processes all video pairs in the same manner. Therefore, we use \tilde{V}'_i to explain the processing steps without loss of generality. The encoder consists of T stacked typical transformer encoder layers, as in [20, 33], producing encoded representations E_{enc} . Our decoder, following [33], also uses T stacked typical transformer decoder layers, along with N learnable moment queries representing the centre m_c and duration m_σ . The decoder processes E_{enc} with the moment queries.

We design prediction heads following [33]. A linear layer predicts saliency scores from the encoded representations, and another linear layer handles negative pairs. From the decoder outputs, a 3-layer MLP with ReLU predicts the normalized moment centre and duration, while a linear layer with softmax predicts the foreground.

Hungarian matching. Following [3, 20, 33], we perform Hungarian matching between the two predictions and two corresponding labels respectively. Give prediction \hat{y} of \tilde{V}'_i and corresponding to ground truth y , the optimal matching results between predictions and ground truths $\hat{\sigma}$ can be written as $\hat{\sigma} = \arg \min_{\sigma \in G_N} \sum_i^N C_{\text{match}}(y, \hat{y}_{\sigma(i)})$, where G is a permutation of predictions and ground truths pairs and C_{match} is the matching cost.

Loss Functions. We calculate the loss between $\hat{\sigma}$ and the ground truth y corresponding to \tilde{V}'_i . Following [20], the L_1 loss \mathcal{L}_{L_1} and the glOU [41] loss \mathcal{L}_{glOU} are used to measure the distance and overlapping between the predictions and a cross-entropy loss \mathcal{L}_{cls} is used to measure classification. For highlight detection, we also use three loss functions which are margin ranking loss \mathcal{L}_{margin} , rank-aware contrastive loss \mathcal{L}_{margin} and negative loss \mathcal{L}_{neg} .

The overall loss is shown as follows with λ_* as balancing

coefficient:

$$\mathcal{L}_{moment} = \lambda_{L_1} \mathcal{L}_{L_1} + \lambda_{iou} \mathcal{L}_{gIoU} + \lambda_{cls} \mathcal{L}_{cls}, \quad (7)$$

$$\mathcal{L}_{hl} = \lambda_{margin} \mathcal{L}_{margin} + \lambda_{cont} \mathcal{L}_{cont} + \lambda_{neg} \mathcal{L}_{neg}, \quad (8)$$

$$\mathcal{L}_{total} = \mathcal{L}_{hl} + \mathcal{L}_{moment}. \quad (9)$$

4. Experiments

4.1. Experimental Setup

Benchmark and evaluation metrics. We evaluate our method on two widely-used benchmarks: QVHighlights [20] and Charades-STA [10]. Following the experimental setup in prior works [20, 33], we provide a comprehensive analysis of the performance of our method.

- The *QVHighlights* dataset consists of over 10,000 video-query pairs, primarily from vlog and news content. For evaluation, we adhere to the *training*, *validation*, and *test* splits as defined in Moment-DETR [20]. We report results for both the *val* and *test* splits.
- The *Charades-STA* dataset is a large-scale benchmark derived from the Charades dataset [44], containing more than 18,000 video-sentence pairs. We follow the standard evaluation protocol, using two separate *training/testing* splits as specified in previous work [10].

To assess the performance of our method, we adopt the evaluation metrics used in Moment-DETR [20]. For Moment Retrieval, we report the mean average precision (mAP) at Intersection over Union (IoU) thresholds of 0.5 and 0.75, as well as the average mAP over IoU thresholds ranging from 0.5 to 0.95 with a step size of 0.05. We also include Recall@1 (R@1) at IoU thresholds of 0.5 and 0.75. For Highlight Detection, we evaluate using both mAP and HIT@1, a clip is considered a positive match if it receives a "Very Good" score. For a fair comparison, we also include the *test* split of the QVHighlights dataset, which is evaluated on the CodaLab competition platform [38]. Notably, performance at higher IoU thresholds, such as 0.7, serves as an indicator of the precision with which predicted moments align with the ground truth.

To further evaluate the robustness of our model, we perform a spurious correlation analysis. Specifically, we replace the target clips in the video content with zero-valued masks while keeping the video duration unchanged. This modification allows us to investigate the potential spurious correlation between the text queries and the video moments. We report *Spurious R@1* and *Spurious mAP* to assess the model’s performance under these conditions, where lower values are indicative of better performance in the presence of spurious correlations. Additionally, we compute the generalized Intersection over Union (gIoU) loss for the three models on the QVHighlights *val* split without zero masks. This provides a measure of the accuracy of moment predictions in the absence of spurious correlations.

Implementation details. Our model is implemented in PyTorch [37]. For all datasets, We use video features both extracted from SlowFast [8] pre-trained on Kinetics [4] and pre-trained CLIP [39] vision encoder, and text feature extracted from pre-trained CLIP [39] text encoder, following the Moment-DETR.

- For *QVHighlights* dataset, we set batch size 32 and an initial learning rate of 1e-4, weight decay 1e-4. We set the hidden size $d = 256$, layers of encoder/decoder $T = 2$, and moment queries $N = 10$. The model is trained for 220 epochs. Loss balancing coefficient are $\lambda_{margin} = 1$, $\lambda_{cont} = 1$, $\lambda_{L_1} = 1$, $\lambda_{gIoU} = 10$, $\lambda_{CE} = 4$ and $\lambda_{neg} = 4$.
- For *Charades-STA*, we set batch size 32 and use an initial learning rate of 2e-4, weight decay 1e-4. We set the hidden size $d = 256$, layers of encoder/decoder $T = 3$, and moment queries $N = 10$. The model is trained for 100 epochs and the learning rate is decayed to 1/10 every 30 epochs. Loss balancing coefficient are $\lambda_{margin} = 1$, $\lambda_{cont} = 1$, $\lambda_{L_1} = 10$, $\lambda_{gIoU} = 1$, $\lambda_{CE} = 4$ and $\lambda_{neg} = 4$.

We use mini-batch and AdamW [31] gradient descent algorithm to optimize the network parameters, initialize weights with Xavier init [14], use dropout of 0.1 for transformer layers and 0.5 for input projection layers and set cost coefficient as the same as loss balancing coefficient on all datasets. For Dynamic Video Synthesizer, the selection Probability α is set to 0.5 and for Dynamic Temporal Identifier the β is set to 0.5 on all datasets. The whole training time on *QVHighlight* is around 8 hours and 6 hours for *Charades-STA* with a single NVIDIA RTX 2080 GPU.

4.2. Quantitative Results

As illustrated in Table 1 and Table 3, we compare *TD-DETR* with several baseline methods in Moment Retrieval.

Results on QVHighlights. On *QVHighlights test* split, we compare our model against proposal-based, proposal-free, and DETR-based methods, as shown in Table 1. As observed, our *TD-DETR* achieves state-of-the-art performance across all evaluation metrics. Notably, *TD-DETR* shows the most significant improvements compared to the other methods. Performance at higher IoU thresholds (*e.g.*, 0.7) provides a clearer indication of the alignment between predicted moments and the ground truth. Our *TD-DETR* outperforms the previous state-of-the-art model by a substantial margin, with improvements of up to 5.98% in R@1@0.7 and 13.8% in mAP@0.75.

Results on Charades-STA. As shown in Table 3, we compare our model with proposal-based, proposal-free and DETR-based methods on *Charades-STA test* split, achieving state-of-the-art performance across all evaluation metrics. Notably, our method achieves improvements of up to 2.36% in R1@0.5 and 11.2% on this challenging bench-

Table 1. Performance comparison on QVHighlights *test* split. Our experiments are averaged over three runs and ‘±’ denotes the standard deviation. For the compared methods, the results are copied from their original papers.

Method	MR-R1		MR-mAP			HD>= Very Good	
	@0.5	@0.7	@0.5	@0.75	Avg.	mAP	HIT@1
MCN [1]	11.41	2.72	24.94	8.22	10.67	-	-
CAL [7]	25.49	11.54	23.40	7.65	9.89	-	-
XML [19]	41.83	30.35	44.63	31.73	32.14	34.49	55.25
XML+ [20]	46.69	33.46	47.89	34.67	34.90	35.38	55.06
Moment-DETR [20]	52.89	33.02	54.82	29.40	30.73	35.69	55.60
MomentDiff [21]	57.42	39.66	54.02	35.73	35.95	-	-
UMT [30]	56.23	41.18	53.83	37.01	36.12	38.18	59.99
QD-DETR [33]	62.40	44.98	62.52	39.88	39.86	38.94	62.40
UniVTG [23]	58.86	40.86	57.60	35.59	35.47	-	-
<i>TD-DETR (Ours)</i>	63.62 _{±0.55}	47.67 _{±0.77}	65.54 _{±0.07}	45.37 _{±0.52}	44.65 _{±0.13}	39.00 _{±0.23}	63.10 _{±0.19}

Table 2. Performance comparison on QVHighlights *val* split with zero masks. We replace the target clips of video content with zeros without changing the duration of the videos. No-training stands for the QD-DETR model without training which we set as the control experiment. We compare the baseline model QD-DETR and our proposed *TD-DETR* in the same settings. The metrics here have been explained in section 4.1

Method	Spurious MR-R1 ↓				Spurious MR-mAP ↓			gIoU loss ↓	Spurious HD>= Very Good ↓	
	@0.3	@0.5	@0.7	mIOU	@0.5	@0.75	Avg.	w/o masks	mAP	HIT@1
(No-training)	24.71	12.19	5.68	20.28	16.25	6.02	7.16	0.94	17.71	19.94
QD-DETR	33.1	28.0	20.39	25.92	29.34	19.96	19.44	0.50	21.68	21.61
<i>TD-DETR (Ours)</i>	18.19	15.61	11.61	14.04	17.0	11.16	10.57	0.39	17.25	12.0

Table 3. Performance comparison on Charades-STA *test* split.

Method	R1@0.5	R1@0.7
CAL [7]	44.90	24.37
2D TAN [62]	39.70	23.31
VSLNet [58]	47.31	30.19
IVG-DCL [34]	50.24	32.88
Moment-DETR [20]	53.63	31.37
Moment-Diff [21]	55.57	32.42
UMT [30]	48.31	29.25
QD-DETR [33]	57.31	32.55
<i>TD-DETR (Ours)</i>	58.66	36.18

mark. Recall that performance at high IoU thresholds stands for the precision with which predictions match the ground truth data.

Results on spurious correlation. Moment retrieval models are often prone to erroneous predictions due to spurious correlations, a typical example being when predictions rely solely on contextual cues. To investigate this issue, we replace the target clips in the video content with zero-value masks while preserving the original video durations. Theoretically, a model that does not rely solely on contextual information should instead focus on semantic and temporal information. In Table 2, we compare the performance of a non-trained model, the baseline model, and our proposed *TD-DETR*. Notably, despite the absence of relevant

scenes, the baseline model still manages to predict the correct moments, suggesting that it is relying solely on spurious cues. In fact, the baseline outperforms early proposal-based models [1, 7] and achieves R@1@0.7 performance nearly on par with the XML model [19]. In contrast, our *TD-DETR* demonstrates minimal reliance on spurious correlations, as evidenced by its superior performance across all evaluation metrics. Note that performance at lower IoU thresholds (e.g., 0.3) highlights the baseline’s tendency to guess the moment location, rather than accurately localizing it. Specifically, *TD-DETR* achieves 45.04% lower *spurious* R@1@0.3 and 45.83% lower *spurious* mIoU compared to the baseline, and 26.39% lower *spurious* R@1@0.3 and 30.8% lower *spurious* mIoU compared to the non-trained model. Additionally, our model achieves the lowest gIoU loss on the official *val* split, outperforming the baseline by 22%. This behavior confirms that our model effectively emphasizes correct causal inference, rather than exploiting context-based cues.

4.3. Qualitative Analysis

In this subsection, we demonstrate the presence of spurious correlations in the baseline model and show how our *TD-DETR* effectively addresses this issue. As illustrated in Figure 4, we replace the video clips corresponding to ground truth moments zero-value masks, which represent noise, and record the predicted moments with the highest confi-

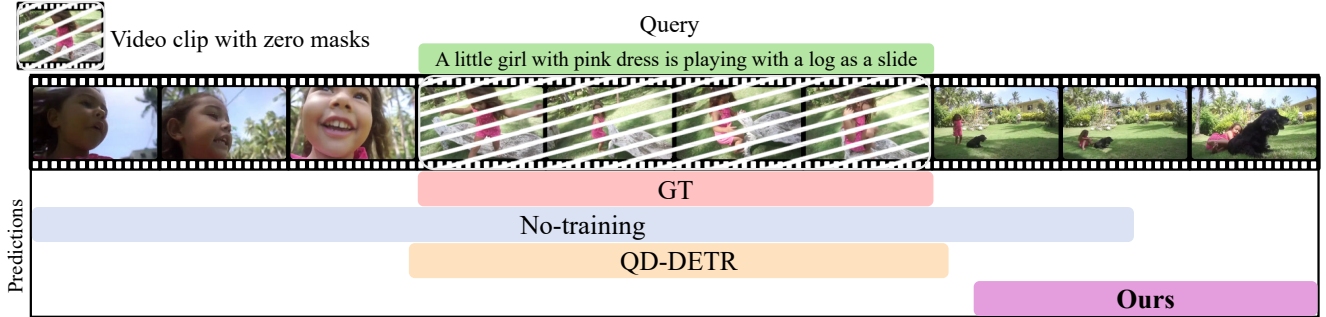


Figure 4. Visualization of results comparison between the no-training model, the baseline model and our *TD-DETR*. Frames with slash means we replace the original content of video clips with zeros. We represent the text query in the green box which is aligned with ground truth moments. We display the relative position of ground truth and prediction moments in colourful boxes, where the pink box with GT stands for ground truth moment, the blue box with no-training stands for prediction of baseline without training, the orange box with QD-DETR stands for our baseline predictions and the purple box with ours stands for our *TD-DETR*. Best read in colour.

Table 4. Ablation study on QVHighlights *val* split. VSDC and TDEM stand for Video Synthesizer for Dynamic Context and Temporal Dynamics Enhancement Module respectively. All the ablation results are averaged over three runs.

	VSDC	TDEM	MR-R1		MR-mAP			HD \geq Very Good	
			@0.5	@0.7	@0.5	@0.75	Avg.	mAP	HIT@1
(a)			61.12	46.77	62.45	43.66	42.54	38.82	62.50
(b)	✓		63.52	49.48	64.88	47.40	45.28	39.12	63.67
(c)		✓	62.95	47.91	64.01	45.38	44.62	38.51	60.80
(d)	✓	✓	65.03	51.07	65.75	48.30	46.97	39.59	64.56

dence. We analyze the results under the condition that the video clips corresponding to the ground truth are replaced with noise. As observed, the non-trained model tends to predict longer spans, suggesting that it is simply guessing the moment locations. In contrast, the baseline model still predicts a precise moment, even when the predicted clip is entirely filled with noise. This indicates that the baseline model relies heavily on contextual cues, rather than the semantic content of the ground truth moments.

On the other hand, our *TD-DETR* model successfully bypasses the noise and predicts the most semantically relevant moments by temporal dynamic learning. For example, when the ground truth is a moment describing “A little girl with pink dress is playing with a log as a slide.”, our model predicts a similar moment “a girl playing with a dog” that partially matches the query with lower confidence. Notably, our model correctly identifies the relevant spans without zero-value masks, which demonstrates its ability to distinguish the semantic and temporal information of the whole video rather than relying on spurious correlations.

4.4. Ablation Studies

As illustrated in Table 4, we perform comprehensive and detailed ablation studies to validate the effectiveness of each proposed component of our work on QVHighlights *val* split. *VSDC* and *TDEM* refer to Video Synthesizer for Dynamic Context and Temporal Dynamics Enhancement

Module, respectively. Rows (b) to (c) show the effectiveness of each component compared to the baseline model (a), and (d) demonstrate the overall effectiveness of all the components. In detail, Video Synthesizer for Dynamic Context contributes improvement of 2.99% in R1@0.7, 2.44% in mAP@0.75 and 4.89% in average mAP while Temporal Dynamics Enhancement Module contributes improvement of 3.93% in R1@0.7, 5.79% in mAP@0.75 and 6.44% in average mAP for Moment Retrieval. With all components integrated, we observe a substantial 9.19%, 10.62% and 10.41% improvement in the R1@0.7, mAP@0.75 and average mAP, respectively, for MR. For further details, we recommend that readers refer to Section 7.1 in the supplementary materials for ablation study on the α and β .

5. Conclusion

Although existing transformer-based approaches have demonstrated remarkable performance, they still struggle with associating the textual query with the background frames rather than the target moment, a problem driven by spurious correlations. To address this issue, we introduce a novel temporal dynamic learning approach. First, we propose a novel video synthesis approach that constructs a dynamic context for the relevant moment. This synthesis mechanism enables our model to attend to the target moment corresponding to the query across various dynamic

contexts. Second, we enhance the representation by learning temporal dynamics. In addition to visual features, text queries are aligned with temporal dynamic representations, allowing our model to establish a robust, non-spurious correlation between the query-related moment and its context. Extensive experiments validate the effectiveness of our *TD-DETR*, demonstrating superior performance and a significant reduction in spurious correlations.

References

- [1] Lisa Anne Hendricks, Oliver Wang, Eli Shechtman, Josef Sivic, Trevor Darrell, and Bryan Russell. Localizing moments in video with natural language. In *ICCV*, pages 5803–5812, 2017. 1, 2, 7
- [2] Sara Beery, Grant Van Horn, and Pietro Perona. Recognition in terra incognita. In *ECCV*, pages 456–473, 2018. 3
- [3] Nicolas Carion, Francisco Massa, Gabriel Synnaeve, Nicolas Usunier, Alexander Kirillov, and Sergey Zagoruyko. End-to-end object detection with transformers. In *ECCV*, pages 213–229. Springer, 2020. 2, 3, 5
- [4] Joao Carreira and Andrew Zisserman. Quo vadis, action recognition? a new model and the kinetics dataset. In *CVPR*, pages 6299–6308, 2017. 6
- [5] Jingyuan Chen, Xinpeng Chen, Lin Ma, Zequn Jie, and Tat-Seng Chua. Temporally grounding natural sentence in video. In *EMNLP*, pages 162–171, 2018. 2
- [6] Victor Escorcia, Mattia Soldan, Josef Sivic, Bernard Ghanem, and Bryan Russell. Temporal localization of moments in video collections with natural language. *arXiv preprint arXiv:1907.12763*, 2019. 2
- [7] Victor Escorcia, Mattia Soldan, Josef Sivic, Bernard Ghanem, and Bryan Russell. Finding moments in video collections using natural language. *arXiv preprint arXiv:1907.12763*, 2019. 7
- [8] Christoph Feichtenhofer, Haoqi Fan, Jitendra Malik, and Kaiming He. Slowfast networks for video recognition. In *ICCV*, pages 6202–6211, 2019. 6
- [9] Valentin Gabeur, Chen Sun, Karteek Alahari, and Cordelia Schmid. Multi-modal transformer for video retrieval. In *ECCV*, pages 214–229. Springer, 2020. 1
- [10] Jiyang Gao, Chen Sun, Zhenheng Yang, and Ram Nevatia. Tall: Temporal activity localization via language query. In *ICCV*, pages 5267–5275, 2017. 2, 6
- [11] Runzhou Ge, Jiyang Gao, Kan Chen, and Ram Nevatia. Mac: Mining activity concepts for language-based temporal localization. In *WACV*, pages 245–253. IEEE, 2019. 2
- [12] Robert Geirhos, Patricia Rubisch, Claudio Michaelis, Matthias Bethge, Felix A Wichmann, and Wieland Brendel. Imagenet-trained cnns are biased towards texture; increasing shape bias improves accuracy and robustness. *ICLR*, 2019. 3
- [13] Soumya Suvra Ghosal and Yixuan Li. Are vision transformers robust to spurious correlations? *IJCV*, 132(3):689–709, 2024. 3
- [14] Xavier Glorot and Yoshua Bengio. Understanding the difficulty of training deep feedforward neural networks. In *AISTATS*, 2010. 6
- [15] Karan Goel, Albert Gu, Yixuan Li, and Christopher Ré. Model patching: Closing the subgroup performance gap with data augmentation. *ICLR*, 2021. 3
- [16] Jinhyun Jang, Jungin Park, Jin Kim, Hyeongjun Kwon, and Kwanghoon Sohn. Knowing where to focus: Event-aware transformer for video grounding. In *ICCV*, pages 13846–13856, 2023. 3
- [17] Minjoon Jung, Youwon Jang, Seongho Choi, Joochan Kim, Jin-Hwa Kim, and Byoung-Tak Zhang. Background-aware moment detection for video moment retrieval, 2025. 2
- [18] Pilhyeon Lee and Hyeran Byun. Bam-detr: Boundary-aligned moment detection transformer for temporal sentence grounding in videos. In *ECCV*, pages 220–238. Springer, 2024. 2, 3
- [19] Jie Lei, Licheng Yu, Tamara L Berg, and Mohit Bansal. Tvr: A large-scale dataset for video-subtitle moment retrieval. In *ECCV*, pages 447–463. Springer, 2020. 2, 7
- [20] Jie Lei, Tamara L Berg, and Mohit Bansal. Detecting moments and highlights in videos via natural language queries. *NeurIPS*, 34:11846–11858, 2021. 2, 3, 4, 5, 6, 7, 1
- [21] Pandeng Li, Chen-Wei Xie, Hongtao Xie, Liming Zhao, Lei Zhang, Yun Zheng, Deli Zhao, and Yongdong Zhang. Momentdiff: Generative video moment retrieval from random to real. *NeurIPS*, 36, 2024. 7
- [22] Chuming Lin, Chengming Xu, Donghao Luo, Yabiao Wang, Ying Tai, Chengjie Wang, Jilin Li, Feiyue Huang, and Yanwei Fu. Learning salient boundary feature for anchor-free temporal action localization. In *CVPR*, pages 3320–3329, 2021. 2
- [23] Kevin Qinghong Lin, Pengchuan Zhang, Joya Chen, Shraman Pramanick, Difei Gao, Alex Jinpeng Wang, Rui Yan, and Mike Zheng Shou. Univt: Towards unified video-language temporal grounding. In *ICCV*, pages 2794–2804, 2023. 7
- [24] Tsung-Yi Lin, Piotr Dollár, Ross Girshick, Kaiming He, Bharath Hariharan, and Serge Belongie. Feature pyramid networks for object detection. In *CVPR*, pages 2117–2125, 2017. 2
- [25] Daizong Liu, Xiaoye Qu, Jianfeng Dong, Pan Zhou, Yu Cheng, Wei Wei, Zichuan Xu, and Yulai Xie. Context-aware biaffine localizing network for temporal sentence grounding. In *CVPR*, pages 11235–11244, 2021. 2
- [26] Meng Liu, Xiang Wang, Liqiang Nie, Xiangnan He, Baoquan Chen, and Tat-Seng Chua. Attentive moment retrieval in videos. In *SIGIR*, pages 15–24, 2018. 2
- [27] Meng Liu, Xiang Wang, Liqiang Nie, Qi Tian, Baoquan Chen, and Tat-Seng Chua. Cross-modal moment localization in videos. In *ACM MM*, pages 843–851, 2018. 2
- [28] Meng Liu, Xiang Wang, Liqiang Nie, Qi Tian, Baoquan Chen, and Tat-Seng Chua. Cross-modal moment localization in videos. In *ACM MM*, pages 843–851, 2018. 3
- [29] Shilong Liu, Feng Li, Hao Zhang, Xiao Yang, Xianbiao Qi, Hang Su, Jun Zhu, and Lei Zhang. Dab-detr: Dynamic anchor boxes are better queries for detr. In *ICLR*, 2022.
- [30] Ye Liu, Siyuan Li, Yang Wu, Chang-Wen Chen, Ying Shan, and Xiaohu Qie. Umt: Unified multi-modal transformers for joint video moment retrieval and highlight detection. In *CVPR*, pages 3042–3051, 2022. 2, 3, 7

- [31] Ilya Loshchilov and Frank Hutter. Decoupled weight decay regularization. In *ICLR*, 2019. 6
- [32] Chujie Lu, Long Chen, Chile Tan, Xiaolin Li, and Jun Xiao. Debug: A dense bottom-up grounding approach for natural language video localization. In *EMNLP-IJCNLP*, pages 5144–5153, 2019. 2
- [33] WonJun Moon, Sangeek Hyun, SangUk Park, Dongchan Park, and Jae-Pil Heo. Query-dependent video representation for moment retrieval and highlight detection. In *CVPR*, pages 23023–23033, 2023. 2, 3, 4, 5, 6, 7, 1
- [34] Guoshun Nan, Rui Qiao, Yao Xiao, Jun Liu, Sicong Leng, Hao Zhang, and Wei Lu. Interventional video grounding with dual contrastive learning. In *CVPR*, 2021. 7
- [35] OpenAI. Video generation models as world simulators, 2024. 1
- [36] Mayu Otani, Yuta Nakashima, Esa Rahtu, and Janne Heikkilä. Uncovering hidden challenges in query-based video moment retrieval. *BMVC*, 2020. 3
- [37] Adam Paszke, Sam Gross, Francisco Massa, Adam Lerer, James Bradbury, Gregory Chanan, Trevor Killeen, Zeming Lin, Natalia Gimelshein, Luca Antiga, et al. Pytorch: An imperative style, high-performance deep learning library. *NeurIPS*, 32, 2019. 6
- [38] Adrien Pavao, Isabelle Guyon, Anne-Catherine Letournel, Dinh-Tuan Tran, Xavier Baro, Hugo Jair Escalante, Sergio Escalera, Tyler Thomas, and Zhen Xu. Codalab competitions: An open source platform to organize scientific challenges. *JMLR*, 24(198):1–6, 2023. 6
- [39] Alec Radford, Jong Wook Kim, Chris Hallacy, Aditya Ramesh, Gabriel Goh, Sandhini Agarwal, Girish Sastry, Amanda Askell, Pamela Mishkin, Jack Clark, et al. Learning transferable visual models from natural language supervision. In *ICML*, pages 8748–8763. PMLR, 2021. 6
- [40] Michaela Regneri, Marcus Rohrbach, Dominikus Wetzal, Stefan Thater, Bernt Schiele, and Manfred Pinkal. Grounding action descriptions in videos. *Trans. Assoc. Comput. Linguistics*, 1:25–36, 2013. 2
- [41] Hamid Rezaatfighi, Nathan Tsoi, JunYoung Gwak, Amir Sadeghian, Ian Reid, and Silvio Savarese. Generalized intersection over union: A metric and a loss for bounding box regression. In *CVPR*, pages 658–666, 2019. 5
- [42] Shiori Sagawa, Pang Wei Koh, Tatsunori B Hashimoto, and Percy Liang. Distributionally robust neural networks for group shifts: On the importance of regularization for worst-case generalization. *arXiv preprint arXiv:1911.08731*, 2019. 3
- [43] Dian Shao, Yu Xiong, Yue Zhao, Qingqiu Huang, Yu Qiao, and Dahua Lin. Find and focus: Retrieve and localize video events with natural language queries. In *ECCV*, pages 200–216, 2018. 2
- [44] Gunnar A Sigurdsson, Gül Varol, Xiaolong Wang, Ali Farhadi, Ivan Laptev, and Abhinav Gupta. Hollywood in homes: Crowdsourcing data collection for activity understanding. In *ECCV*, pages 510–526. Springer, 2016. 6
- [45] Lifu Tu, Garima Lalwani, Spandana Gella, and He He. An empirical study on robustness to spurious correlations using pre-trained language models. *ACL*, 8:621–633, 2020. 3
- [46] Yipei Wang and Xiaoqian Wang. On the effect of key factors in spurious correlation: A theoretical perspective. In *AISTATS*, pages 3745–3753. PMLR, 2024. 3
- [47] Zhao Wang and Aron Culotta. Identifying spurious correlations for robust text classification. *EMNLP*, 2020. 3
- [48] Fanyue Wei, Biao Wang, Tiezheng Ge, Yuning Jiang, Wen Li, and Lixin Duan. Learning pixel-level distinctions for video highlight detection. In *CVPR*, pages 3073–3082, 2022. 1
- [49] Shaoning Xiao, Long Chen, Songyang Zhang, Wei Ji, Jian Shao, Lu Ye, and Jun Xiao. Boundary proposal network for two-stage natural language video localization. In *AAAI*, pages 2986–2994, 2021. 2
- [50] Huijuan Xu, Kun He, Bryan A Plummer, Leonid Sigal, Stan Sclaroff, and Kate Saenko. Multilevel language and vision integration for text-to-clip retrieval. In *AAAI*, pages 9062–9069, 2019.
- [51] Mengmeng Xu, Mattia Soldan, Jialin Gao, Shuming Liu, Juan-Manuel Pérez-Rúa, and Bernard Ghanem. Boundary-denoising for video activity localization. *arXiv preprint arXiv:2304.02934*, 2023. 2
- [52] Yifang Xu, Yunzhuo Sun, Yang Li, Yilei Shi, Xiaoxiang Zhu, and Sidan Du. Mh-detr: Video moment and highlight detection with cross-modal transformer. In *ACM MM*, 2023. 3
- [53] Jin Yang, Ping Wei, Huan Li, and Ziyang Ren. Task-driven exploration: Decoupling and inter-task feedback for joint moment retrieval and highlight detection. In *CVPR*, pages 18308–18318, 2024. 2, 3
- [54] Yitian Yuan, Lin Ma, Jingwen Wang, Wei Liu, and Wenwu Zhu. Semantic conditioned dynamic modulation for temporal sentence grounding in videos. *NeurIPS*, 32, 2019. 2
- [55] Yitian Yuan, Lin Ma, Jingwen Wang, Wei Liu, and Wenwu Zhu. Semantic conditioned dynamic modulation for temporal sentence grounding in videos. In *Neurips*, 2019. 2
- [56] Runhao Zeng, Haoming Xu, Wenbing Huang, Peihao Chen, Mingkui Tan, and Chuang Gan. Dense regression network for video grounding. In *CVPR*, pages 10287–10296, 2020. 2
- [57] Da Zhang, Xiyang Dai, Xin Wang, Yuan-Fang Wang, and Larry S Davis. Man: Moment alignment network for natural language moment retrieval via iterative graph adjustment. In *CVPR*, pages 1247–1257, 2019. 2
- [58] Hao Zhang, Aixin Sun, Wei Jing, and Joey Tianyi Zhou. Span-based localizing network for natural language video localization. In *ACL*, 2020. 7
- [59] Hao Zhang, Aixin Sun, Wei Jing, and Joey Tianyi Zhou. Temporal sentence grounding in videos: A survey and future directions. *IEEE TPAMI*, 45(8):10443–10465, 2023. 1, 2, 3
- [60] Michael Zhang, Nimit S Sohoni, Hongyang R Zhang, Chelsea Finn, and Christopher Ré. Correct-n-contrast: A contrastive approach for improving robustness to spurious correlations. *ICML*, 2022. 3
- [61] Songyang Zhang, Jinsong Su, and Jiebo Luo. Exploiting temporal relationships in video moment localization with natural language. In *ACM MM*, pages 1230–1238, 2019. 2
- [62] Songyang Zhang, Houwen Peng, Jianlong Fu, and Jiebo Luo. Learning 2d temporal adjacent networks for moment local-

- ization with natural language. In *AAAI*, pages 12870–12877, 2020. [2](#), [7](#)
- [63] Xing Zhang, Zuxuan Wu, Zejia Weng, Huazhu Fu, Jingjing Chen, Yu-Gang Jiang, and Larry S Davis. Videolt: Large-scale long-tailed video recognition. In *ICCV*, pages 7960–7969, 2021. [3](#)
- [64] Yifan Zhang, Bingyi Kang, Bryan Hooi, Shuicheng Yan, and Jiashi Feng. Deep long-tailed learning: A survey. *IEEE TPAMI*, 45(9):10795–10816, 2023. [3](#)
- [65] Zhu Zhang, Zhijie Lin, Zhou Zhao, and Zhenxin Xiao. Cross-modal interaction networks for query-based moment retrieval in videos. In *ACM SIGIR*, pages 655–664, 2019. [2](#)
- [66] Yue Zhao, Yuanjun Xiong, Limin Wang, Zhirong Wu, Xiaoou Tang, and Dahua Lin. Temporal action detection with structured segment networks. In *ICCV*, pages 2914–2923, 2017. [2](#)
- [67] Xizhou Zhu, Weijie Su, Lewei Lu, Bin Li, Xiaogang Wang, and Jifeng Dai. Deformable detr: Deformable transformers for end-to-end object detection. In *ICLR*, 2021. [3](#)

The Devil is in the Spurious Correlation: Boosting Moment Retrieval via Temporal Dynamic Learning

Supplementary Material

In this supplementary material, we elaborate on the details of the network structure, learning objectives, and analysis of sensitiveness on the hyper-parameters of the proposed method.

6. Details of Network and Objectives

In this section, we present our network and loss functions in detail.

Transformer encoder-decoder with prediction heads. We follow the architectural principles outlined in [20, 33] for the design of our transformer and prediction heads, with modifications introduced in the encoder. Specifically, we integrate our proposed *Temporal Dynamic Tokenizer* into the encoder to address spurious correlations effectively.

Given a spurious pair $p'_i = \{\tilde{V}'_i, \tilde{V}'_{k_i}\}$, this module processes all video pairs uniformly. As introduced in Section 3.2, we use T to denote the temporal dynamics. To incorporate these dynamics, we employ two transformer encoder layers with cross attention that facilitate bidirectional interactions: (1) between the temporal dynamics and the text query, and (2) between the video content and the text query. Once the temporal dynamics and video content are individually aligned with the text, we apply a weighted element-wise addition to combine their outputs. This rejected representation is subsequently processed through a standard transformer layer to refine the contextual understanding. Given a spurious pair $p_i = \{\tilde{V}_i, \tilde{V}_{k_i}\}$, our approach generates a refined spurious pair $p'_i = \{\tilde{V}'_i, \tilde{V}'_{k_i}\}$ that incorporates these temporal and semantic enhancements.

Loss Functions. We compute the loss between the predicted output \hat{y} and its corresponding ground truth y (m_i) for \tilde{V}_i , as well as between \hat{y}' and its ground truth y' (m'_i) for \tilde{V}_{k_i} . The predictions are matched with their targets, and the loss is calculated using L1 loss, generalized IoU (gIoU) loss, and cross-entropy loss, respectively, as described in [20].

7. Sensitiveness Analysis

7.1. Video Synthesizer for Dynamic Context

In Section 3.1, we construct a new sample \tilde{V}_{k_i} with dynamic context from spurious pair $p_i = \{V_i, V_{k_i}\}$ as follows,

$$\tilde{V}_{k_i} = \alpha \cdot V_i + (1 - \alpha) \cdot V_{k_i}, \quad (10)$$

where α represents the sampling ratio of V_i while $1 - \alpha$ corresponds to V_{k_i} .

Table S1. Sensitiveness analysis of sampling ratio α on QVHighlights *val* split.

α	MR-R1		MR-mAP			HD \geq Very Good	
	@0.5	@0.7	@0.5	@0.75	Avg.	mAP	HIT@1
0.1	64.52	50.26	65.56	48.13	46.47	39.13	62.32
0.3	66.00	50.71	65.51	46.61	46.16	39.85	64.06
0.5	65.03	51.07	65.75	48.30	46.97	39.59	64.56
0.7	64.45	50.00	64.61	45.88	45.52	38.93	61.87
0.9	62.84	49.68	63.30	44.65	44.34	38.51	60.65
1.0	62.95	47.91	64.01	45.38	44.62	38.51	60.80

Table S2. Sensitiveness analysis of sampling ratio β on QVHighlights *val* split.

β	MR-R1		MR-mAP			HD \geq Very Good	
	@0.5	@0.7	@0.5	@0.75	Avg.	mAP	HIT@1
0.1	64.26	49.42	65.35	47.04	45.60	39.06	63.48
0.3	64.65	51.23	65.55	47.24	46.16	39.64	64.45
0.5	65.35	51.10	66.16	47.50	46.71	39.59	64.56
0.7	64.90	51.55	65.73	47.22	46.83	39.36	63.68
0.9	64.84	51.35	65.96	48.68	47.30	39.74	63.29
1.0	63.52	49.48	64.88	47.40	45.28	39.12	63.67

We examine the impact of the sampling ratio α on the quality of the synthesized samples. In detail, we adapt α ranging from 0.1 to 0.9 with a step size of 0.2.

As illustrated in Table S1, when the sampling ratio α increases, the synthesized video incorporates more tokens from the videos containing the target moments with corresponding dynamic contexts, thus improving the performance of moment retrieval. The performance starts to decline from $\alpha = 0.7$, due to the lack of dynamics of the contexts. Specifically, when $\alpha = 1.0$, the synthesized video is identical to the original video. This ablation study on α demonstrates the effectiveness of our *Video Synthesizer for Dynamic Context* in improving model performance by balancing contextual information and target moment focus. Besides, even with various sampling ratios α , our method still achieves promising results, which demonstrate the robustness of the proposed method.

7.2. Temporal Dynamics Enhancement

In section 3.2, the model learns from both dynamic and video information via cross-attention machines. To emphasize the learned dynamic information, we inject text-guided

dynamic representation T' into video \tilde{V}_i as follows,

$$\tilde{V}'_i = \beta \cdot \tilde{V}_i + (1 - \beta) \cdot V_i, \quad (11)$$

where β represents the injection ratio of the video information we used, while $1 - \beta$ corresponds to temporal information T' . We also examine the impact of the injection ratio β on the quality of the injected videos. In detail, we adapt β ranging from 0.1 to 0.9 with a step size of 0.2. As illustrated in Table S2, when the injection ratio β decreases, the video is injected with more temporal information, thus improving the performance of moment retrieval. The performance achieves the highest performance when $\beta = 0.9$, which indicates the benefits of dynamic enhancement. Specifically, when $\beta = 1.0$, no dynamic information is injected into the video, thus the performance drops a lot in contrast to those with dynamics representation. Note that even if $\beta = 0.1$, the model performs well. This ablation study on β validates the effectiveness of our *Temporal Dynamics Enhancement* in boosting moment retrieval by encouraging our model to align text queries with temporal-dynamic representations. Besides, even with various sampling ratios β , our method still achieves promising results, which demonstrate the robustness of the proposed method.